Synchronism and Direction Detection in High-Resolution/High-Density Electromagnetic Encoders

Cristian Herrojo, *Member, IEEE*, Ferran Paredes, *Member IEEE*, and Ferran Martín, *Fellow, IEEE*

***Abstract*—Recently, electromagnetic encoders with synchronous reading and direction detection capability have been reported. Such structures are useful for the implementation of (i) displacement/velocity sensors and (ii) chipless-RFID systems based on near-field coupling and sequential bit reading. In the latter, synchronous reading and motion direction detection are a need in order to avoid false readings of the identification (ID) code, if the relative velocity between the reader and the encoder is not constant, and to read the correct ID code (rather than the inverse one), respectively. On the other hand, synchronous reading and motion direction detection, are essential to determine the encoder direction in displacement/velocity sensors, as well as to provide the absolute position of the encoder, provided that the whole encoder is encoded with the Bruijn sequence. In this paper, synchronous reading and direction detection in high-resolution/high-density electromagnetic encoders based on chains of linearly-shaped metallic inclusions are reported. To this end, it is necessary to add two chains of metallic inclusions to the one containing the ID code. In the reader side, three harmonic signals are necessary in order to generate the clock signals and to obtain the ID code. The reader consists of a microstrip line loaded with three pairs of open-ended folded stubs positioned face-to-face by their extremes. By displacing the encoder chains over the extreme of the stubs, at short distance, stub coupling is enhanced when a metallic inclusion lies on top of the stubs, and the frequency response of the reader is shifted towards lower frequencies. Thus, by injecting three (properly tuned) harmonic signals at the input port of the microstrip transmission line, three amplitude modulated (AM) signals are generated by tag motion at the output port of such transmission line, and the envelope functions contain the velocity, the ID code and the absolute position. The reported reader/encoder system exhibits superior space resolution and information density as compared to other similar systems based on synchronous reading.**

***Index Terms*—Chipless-RFID, electromagnetic encoders, microstrip technology, microwave sensors.**

I. Introduction

ELECTROMAGNETIC (or microwave) encoders may constitute a good alternative to optical encoders [1]-[3] in scenarios subjected to harsh and hostile conditions (i.e., with pollution, dirtiness, grease, etc.). Such conditions are typical in many mechanical systems where an accurate control of the position and velocity of their moving parts is essential (servomotors, elevators, pointing mechanisms, conveyor belts, etc.). Thus, electromagnetic encoders are of interest for motion control applications, as low-cost displacement and velocity sensors able to operate under extreme conditions, not optimal for their optical counterparts [4]-[8].

It has also been demonstrated that electromagnetic encoders can be applied to the implementation of high-data density (and capacity) chipless-RFID systems based on near-field coupling between the reader and the tag (the encoder) and sequential bit reading [9]-[19]. In such application, two relevant advantages, as compared to other chipless-RFID systems based on frequency domain [20]-[52], can be highlighted: (i) the virtually null bandwidth of the interrogation signal (a single-tone harmonic signal), representing a significant cost reduction in the reader side; (ii) the highly achievable data capacity (only limited by the encoder, or tag, size), related to the fact that the bits are read sequentially by displacing the tag over the sensitive part of the reader at short distance. By contrast, in frequency-domain chipless-RFID systems, wideband interrogation signals are required, since the tags consist of a set of resonant elements tuned to different frequencies. Moreover, the data capacity in such systems is typically small (or moderate), since the interrogation signal can cover only a limited spectral bandwidth. The main limitation of these chipless-RFID systems is the requirement of tag alignment and proximity with the reader. However, this near-field system operation does not represent a penalty in certain applications, especially those devoted to security and authentication, where tag reading by proximity guarantees major system confidence against spying and eavesdropping. Secure paper, anti-counterfeiting of premium products, etc., are some potential applications of these near-field chipless-RFID systems based on microwave encoders [9]. Note that laminated encoders with buried metallic inclusions can be also implemented, thereby offering further levels of security against copying or spying by direct sight. Nevertheless, for authentication applications, the key aspect is

This work was supported by MICIIN-Spain (project TEC2016-75650-R and PID2019-103904RB-I00), by *Generalitat de Catalunya* (project 2017SGR-1159), by *Institució Catalana de Recerca i Estudis Avançats* (who awarded Ferran Martín), and by FEDER funds.

C. Herrojo, F. Paredes, and F. Martín are with GEMMA/CIMITEC, Departament d'Enginyeria Electrònica, Universitat Autònoma de Barcelona, 08193 Bellaterra, Spain. E-mail: Ferran.Martin@uab.es.

the reproducibility of the encoders, not easy in both laminated and bare encoders.

In the electromagnetic encoders reported in [4],[5], implemented as circular periodic chains of metallic resonators and aimed to the accurate measurement of angular displacements and velocities, the rotation angle is determined from the cumulative number of pulses from a reference (REF) position, whereas the instantaneous velocity is inferred from the time lapse between adjacent pulses (provided the period of the encoder chain is well known). These incremental-type encoders exhibit a fundamental limitation, i.e., if a reset occurs, the information relative to the angular position is lost. In other words, the encoders reported in [4],[5] do not provide the absolute position, as most optical encoders do. These encoders consist of periodic chains, with all the resonant elements present at their predefined positions.

By contrast, microwave encoders used as chipless-RFID tags are implemented by means of coded sequences, achieved by the presence or absence of functional (operative) resonators, or inclusions, at their predefined positions in the encoder chain [9]. In such application, an *N*-bit chipless tag is read by displacing it over the sensitive part of the reader, which provides the ID code sequentially, bit by bit. In this case, a constant, and well-known, relative velocity between the tag and the reader is necessary, in order to avoid false readings. The encoder velocity can be determined by means of header bits [11],[13], but a uniform velocity may not be guaranteed in certain applications. Thus, to provide system robustness against potential velocity variations, a clock signal, for synchronization, is required.

According to the previous words, adding a periodic chain to near-field chipless-RFID tags is necessary in order to generate a clock signal that prevents from false readings (related to uncertainties in the relative velocity between the tag and the reader). Thus, system synchronism dictating the instants of time for sequentially reading the bits of the encoder is very convenient. Nevertheless, the motion direction, and hence the correct ID code of the encoder cannot be extracted by using only a single clock chain. Note that, if the ID code is not symmetric, the reading direction must be known. Preliminary results of electromagnetic encoders with synchronous reading have been recently reported by the authors by implementing the encoders with chains of square or rectangular metallic patches. In [53]-[55], a single chain of patches is considered, and the ID code is given by the patch size (the clock signal being generated by tag motion over the reader). By contrast, in [56], two independent chains are considered, one for the ID code (the binary states given by the presence or absence of patch), and another one for the clock signal, which provides also the velocity. This latter system is useful to determine the direction of motion. However, in the systems reported in [53]-[56], the encoder resolution (system used as position sensor) and the data density per surface (system functionality as chipless-RFID tag), are limited due to patch size and spacing (period).

In this paper, synchronous reading in electromagnetic encoders (either devoted to position/velocity sensors or as chipless-RFID tags), based on linearly shaped inclusions, is introduced. Such inclusions are very narrow and oriented in the direction orthogonal to axis of the tag chain, thereby representing a good solution in terms of data density and resolution. The main challenge of this work is the design of the sensitive part of the reader, able to provide the clock signals as well as the ID code. Indeed, the work is inspired by the structure reported in [16]. The main novelty concerns the fact that for the generation of the clock signal, necessary for synchronous reading, a new sensing element tuned to a different frequency is necessary. Moreover, a prototype able to provide also the direction of motion of the encoder with regard to the reader is also included in this paper. This requires a further sensing element, thereby representing a major challenge from the design viewpoint. The result is an encoder system with synchronous reading and motion direction detection capacity, with very competitive information density and resolution, implemented for the first time with linear metallic strips.

II. Reader and Encoder Design

The strategy for synchronously reading the considered encoders is to implement two chains of metallic inclusions, dedicating one to the ID code, and the other one to the clock signal. Naturally, in the ID chain, encoding is achieved by the presence (‘1’ logic state) or absence (‘0’ logic state) of functional metallic inclusions. By contrast, all the inclusions are present, and hence functional, in the clock chain. Nevertheless, for displacement direction detection, the encoder must be implemented by etching three chains of metallic inclusions in the tag substrate. One of such chains contains the ID code, whereas from the other two, it is possible to infer the velocity and motion direction, as it will be shown next. In this paper, a synchronous reader/encoder system is first presented, and then the motion direction detection capability is introduced in a new prototype.

A. Synchronous Reader for Encoders Based on Linear Metallic Strips

The working principle of the proposed system based on electromagnetic encoders with synchronous reading is depicted in Fig. 1. According to this sketch, a combiner should be connected to the input port of the sensitive part of the reader in order to inject the two required harmonic signals (interrogation signals). On the other hand, in order to separately obtain the clock signal and the ID code, an inverse scheme (based on a duplexer) is applied to the output port, as it can be appreciated in Fig. 1. Such system is similar to the one presented in [16]. However, in the work presented in this paper, the reader is a microstrip transmission line loaded with two pairs of folded open-ended stubs. The layout of the reader/encoder structure is depicted in Fig. 2. In [16], an unprecedented per-unit-length and per-unit-surface data density in chipless RFID systems based on near-field coupling and sequential bit reading was achieved. The reader used a single pair of identical folded open-ended stubs. Such structure exhibits a single transmission zero at the frequency where the stub length is a quarter-wavelength, as expected. Despite the fact that the extremes of the stubs are face-to-face, inter-stub coupling is negligible. However, when a metallic strip is located on top of the extremes of the stubs, at short distance, inter-stub coupling increases and the transmission zero splits. Furthermore, the reader designed in [16] exhibits a reflection zero, whose frequency position

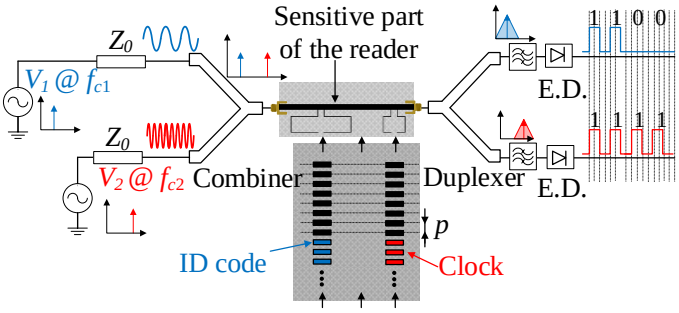

Fig. 1. Sketch showing the working principle of the proposed reader/encoder system based on metallic inclusions and synchronous reading.

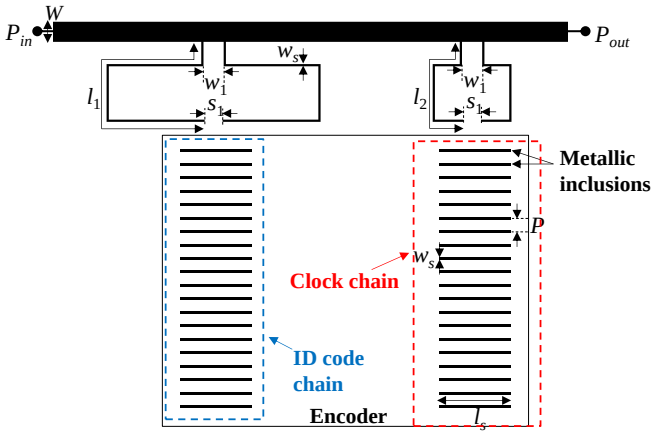

Fig. 2. Layout of reader/encoder structure based on a microstrip transmission line loaded with two pairs of folded open-ended stubs. Dimensions (in mm) are: W = 1.81, l_1 = 24.39, l_2= 12.33, w_1 = 1.80, s_1 = 1.60, P = 1.20, w_s = 0.20 and l_s = 6.40.

depends on the distance between the contact points of the stubs to the host line.

According to the previous words, it is possible to achieve a large excursion of the transmission coefficient by designing the structure so that the reflection zero of the bare reader, f_c, coincides with the first transmission zero, f_z, of the loaded reader, i.e., with a functional metallic inclusion on top of it. Thus, if the reader is fed with a harmonic signal (interrogation signal) tuned to the reflection zero frequency (f_c), an AM modulated signal containing the ID code will be generated at the output port of the microstrip transmission line by tag motion. Such ID code can be extracted from the envelope of the AM signal by means an envelope detector, provided the encoder period is well known and the relative velocity between the sensitive part of the reader and the encoder is constant and well known. However, in the system proposed in [16], if such relative velocity is not constant, a correct bit reading cannot be guaranteed.

In this work, as mentioned before, the sensitive part of the reader of Fig. 2 has been implemented with two different pairs of folded open-ended stubs, thereby providing two transmission zeros and two reflection zeros to the frequency response of the bare reader. Therefore, two independent chains must be considered in order to separately obtain the ID code and the clock signal. In the clock chain, all the metallic inclusions are present at predefined position in order to determine the instants

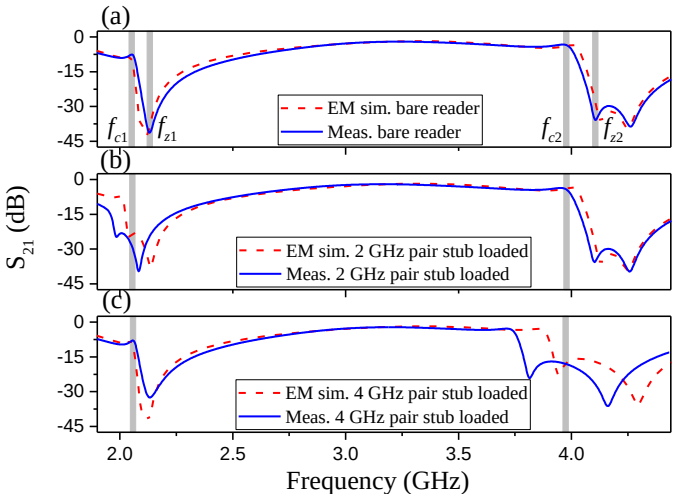

Fig. 3. Electromagnetic simulation (including losses) and measured frequency responses of the: (a) bare reader, (b) reader with the longer stub pair loaded with a metallic strip on top of it, and (c) reader with the shorter stub pair loaded with a metallic strip on top of it.

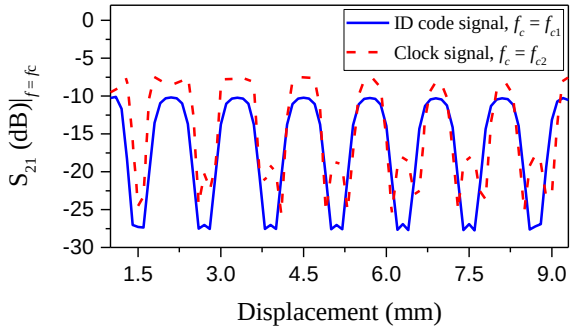

Fig. 4. Variation of the transmission coefficient at the interrogation signal frequencies (f_{c1} and f_{c2}) resulting by displacing 7 metallic elements over the reader. The considered airgap is 0.2 mm. Note that although the maximum transmission is not close to 0 dB, a significant excursion of the transmission coefficient is achieved.

of time for synchronously reading the ID code, as well as the relative velocity (or even acceleration) of the encoder with regard to the sensitive part of the reader.

The reader has been designed in order to exhibit the two reflection zeros, f_{c1} and f_{c2}, in the vicinity of the two transmission zeros, f_{z1} and f_{z2}, (that appear when the corresponding stub length is a quarter-wavelength). Figure 3 plots the lossy electromagnetic simulation, inferred by means of *Keysight ADS*, and the measured response of the: (i) bare reader and (ii) reader with only one stub pair loaded with a metallic inclusion on top of it (two cases). The considered substrate is the *Rogers RO4003C* with dielectric constant ε_r = 3.55, thickness h = 0.81 mm, and loss tangent $\tan\delta$ = 0.0021. For the encoder, the substrate is the same of the reader, but with thickness h = 0.204 mm. Note that, in the transmission coefficient of the bare reader, the transmission zero frequencies are roughly f_{z1} = 2.1 GHz and f_{z2} = 4.2 GHz. Therefore, it is guaranteed that both chains of metallic elements modify only the corresponding transmission zero when the encoder is displaced over the reader, as demonstrated in Fig. 3. On the other hand, by feeding the reader line with two harmonic interrogation signals tuned to f_{c1} =2.02 GHz and f_{c2} = 3.98 GHz, a significant excursion of the transmission coefficient results by

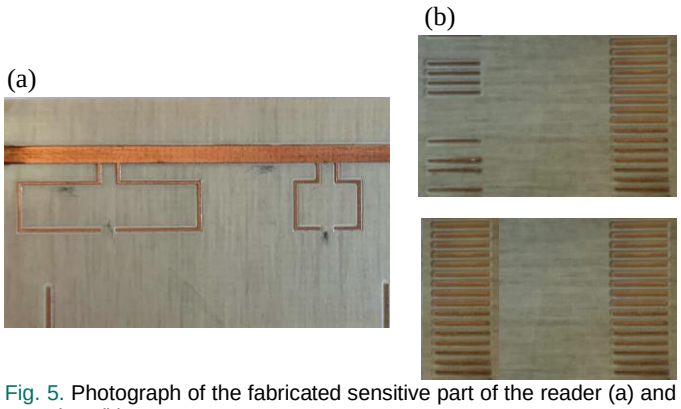

Fig. 5. Photograph of the fabricated sensitive part of the reader (a) and encoders (b).

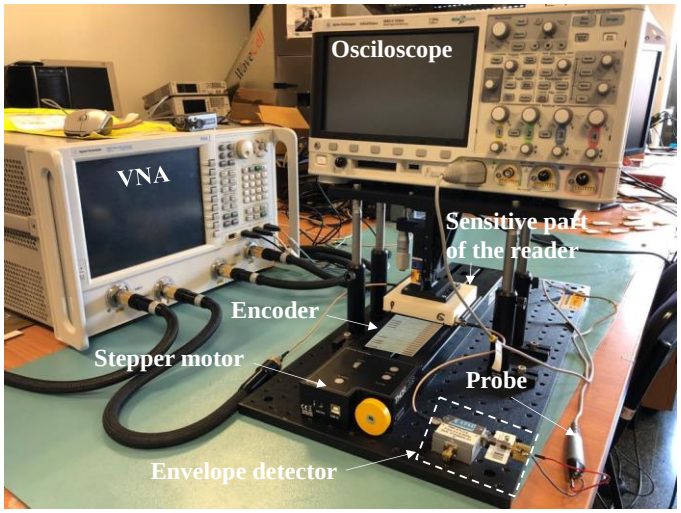

Fig. 6. Photograph of the experimental setup.

tag motion. This can be appreciated in Fig. 4, where the variation of the transmission coefficient at the interrogation signal frequencies (f_{c1} and f_{c2}) has been obtained (by means of simulation) by displacing 7 metallic inclusions over the reader.

For experimental validation, two different 16-bit encoders have been fabricated. The photographs of such encoders and the sensitive part of the reader are depicted in Fig 5. The fabrication has been carried out by means of a LPKF-100 milling machine on the substrate indicated before.

The photograph of the experimental set-up is shown in Fig. 6. The two necessary interrogation signals (tuned to f_{c1} and f_{c2}) to synchronous reading the ID code of the encoder, have been injected independently at the input port of the microstrip transmission line, and we have obtained the envelope signal for each case. Such interrogation signals have been generated by means of a network analyzer (model *Agilent N5221A*), whereas an oscilloscope (model *Agilent MSO-X-3104A*) has been used to visualize the ID code of the encoder. The envelope detector has been implemented by means of a Schottky diode (model *Avago HSMS-* 2860) and the *N2795A* active probe (with capacitance C = 1 pF and resistance R = 1 MΩ). A circulator (model *ATM ATc4-8*) has been used in order to avoid reflections from the Schottky diode. Finally, the relative displacement between the sensitive part of the reader and the encoder has been achieved by means of a linear displacement system (model

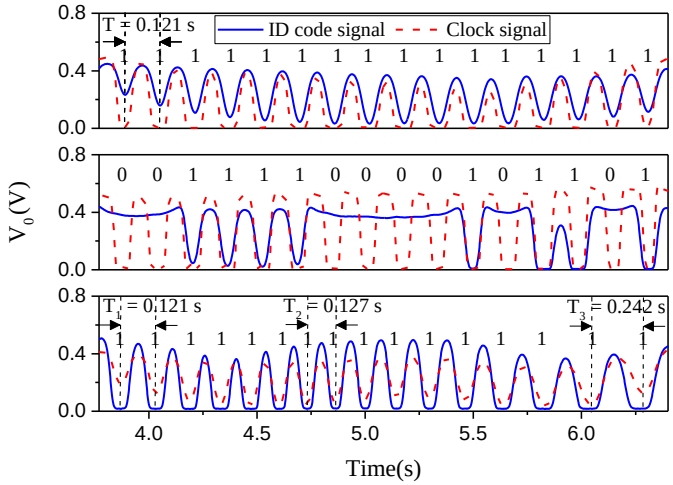

Fig. 7. Measured envelope function of the 16-bit encoders with the indicated codes. The considered airgap is 0.2 mm.

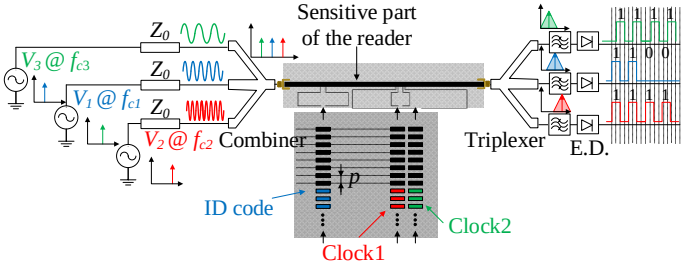

Fig. 8. Sketch showing the working principle of the proposed reader/encoder system based on metallic inclusions and synchronous reading with direction detection capability.

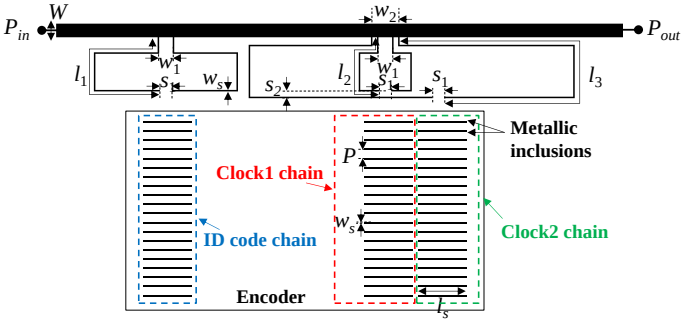

Fig. 9. Layout of reader/encoder structure based on a microstrip transmission line loaded with three pair of folded open-ended stubs. Dimensions (in mm) are: W = 1.81, l_1 = 24.39, l_2= 12.33, l_3= 48.60, w_1 = 1.80, w_2 = 3.40, s_1 = 1.60, s_2 = 0.90, P = 1.20, w_s = 0.20 and l_s = 6.40.

STM 23Q-3AN). Such system allows us to control the vertical distance (air gap) between the sensitive part of the reader and the encoder, the relative velocity, or even the acceleration of the encoder.

With this experimental setup, the measured envelope functions, corresponding to the 16-bit encoders of Fig. 5(b), have been inferred by displacing such encoders over the sensitive part of the reader [see Fig. 5(a)]. As it can be appreciated from Fig. 7(a) and Fig. 7(b), the measured envelope functions, corresponding to ID code and clock signals (which perfectly determine the instants of time for sequentially reading the ID code of the encoder), exhibit dips when a strip is on top of the corresponding stub pair. For the clock signal, the dips

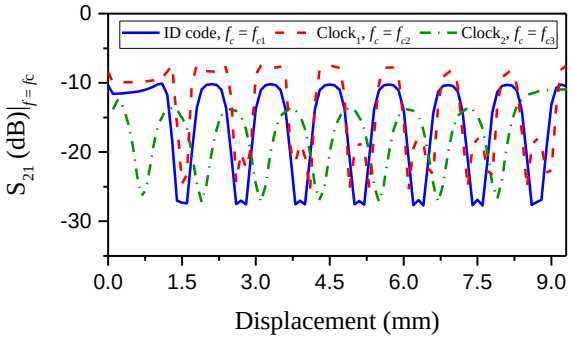

Fig. 10. Variation of the transmission coefficient at the interrogation signal frequencies (f_{c1}, f_{c2} and f_{c3}) resulting by displacing 7 metallic elements over the reader. The considered airgap is 0.2 mm.

appear at periodic time intervals because the velocity of the linear displacement system is constant, i.e., the nominal velocity is 10 mm/s. The displacement velocity that results from the time interval between adjacent peaks, T = 0.121 s, and the encoder period, P = 1.2 mm, is 9.92 mm/s (in good agreement with the nominal value).

As mentioned before, with this synchronous reader/encoder structure, a constant velocity of the encoder with regard to the sensitive part of the reader (in order to read the ID code) is not necessary. To demonstrate this aspect, Fig. 7(c) depicts the measured envelope functions of the encoder with the indicated code [the same one as the Fig.7 (a)], when it is displaced over the sensitive part of the reader with a nominal acceleration of 3 mm/s^2. With this result, it is validated that, regardless of the instantaneous velocity of the encoder with regard to the sensitive part of the reader, the ID code of the encoder can be extracted. Nevertheless, note that, with the synchronous reader/encoder structure presented in this section, it is not possible to distinguish the direction of the encoder, and hence, it is not possible to guarantee the reading of the proper ID code.

B. Synchronous Reader with direction detection for Encoders Based on Linear Metallic Strips

As aforementioned, with the structure presented in the previous section, it is not possible to determine the motion direction. To this end, it is necessary to provide a redundant clock signal by adding a third folded open-ended stub pair in the sensitive part of the reader, and a third strip chain in the encoder (with all metallic inclusions present). By these means, a third transmission zero, f_{z3}, and reflection zero, f_{c3}, is added to the frequency response of the bare reader. Obviously, to determine the motion direction, the reader must be fed with a third harmonic (interrogation) signal tuned to f_{c3}, which will be AM modulated by tag motion at the output port of the microstrip transmission line. The sketch of the working principle and layout of the reader/encoder structure are depicted in Fig. 8 and Fig. 9, respectively. Note that the period of both clock chains is identical. Nevertheless, the fact that such period does not coincide with the distance s_2 (see Fig. 9) implies that one clock signal will be lagged or leaded with regard to the other. Such aspect can be seen in Figure 10, where a variation of the transmission coefficient at the interrogation signal (f_{c1} = 2.02 GHz, f_{c2} = 3.98 GHz and f_{c3} = 0.959 GHz) has been obtained (by means of simulation) by displacing 7 metallic inclusions over the reader. Thus, by using two clock signals, the

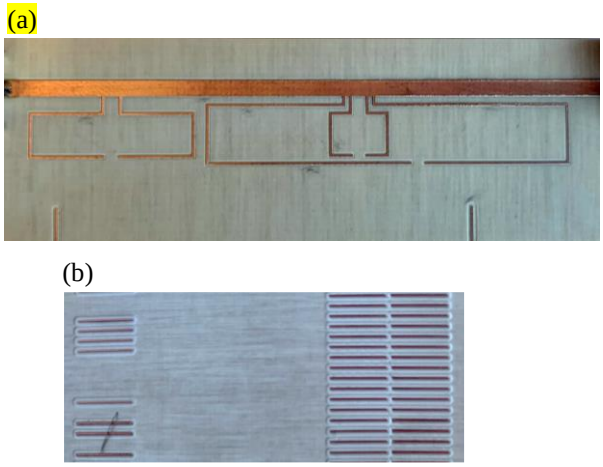

Fig. 11. Photograph of the fabricated sensitive part of the reader (a) and the encoder (b).

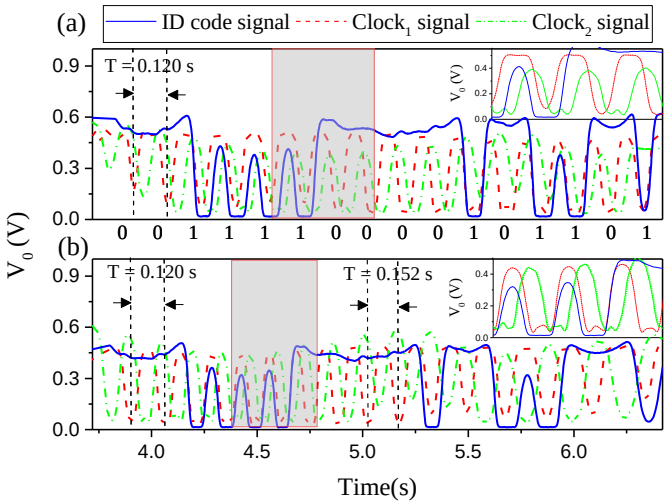

Fig. 12. Measured envelope function of the 16-bit encoder with the indicated code by considering encoder motion with (a) constant velocity and (b) constant acceleration. The considered airgap is 0.2 mm.

displacement direction, and hence the correct ID code, can be inferred.

On the other hand, it is also possible to provide the absolute position of the encoder. Such absolute position can be determined by using the Bruijn sequence [57], which guarantees that any N-bit sub-code does not repeat for the total set of different positions of the encoder [56]. Therefore, it is necessary to read a bit of the coded chain, at a determined position, plus the previous N-1 bits in order to obtain the absolute position of the encoder. If L is the total length of the encoder and p is the distance between adjacent strips (period, or spatial resolution), the total number of different positions is thus L/p. Consequently, the number of bits of the sub-code required to unambiguously determine the encoder position must satisfy

$$N \geq \log_2\left(\frac{L}{p}\right) \quad (1)$$

For instance, for an encoder length of L = 1 m, and period of p = 1.20 mm, N = 10 bits suffice to determine the position. Note

that the system must incorporate a table with the position assigned to the different *N*-bit sub-code sequences, and this is necessary for both motion directions. Naturally, after a system reset, it is necessary that the encoder moves *N* strip positions in order to read the necessary *N* bits of the sub-code. For this main reason it is reasonable to consider that the proposed system is able to provide the quasi-absolute (rather than absolute) position of the encoder.

For validation purposes, a 16-bit encoder ($N = 4$), with a specific De Bruijn sequence, has been fabricated. The photographs of such encoder and sensitive part of the reader are depicted in Fig 11. It must be pointed out that the encoder and the sensitive part of the reader have been implemented on the same substrate as the one used in the synchronous reader/encoder structure presented in the previous section, and measured with the experimental setup shown in Fig. 6.

The three measured envelope functions of the fabricated encoder, by considering constant velocity as well as constant acceleration of the encoder with regard to the sensitive part of the reader, are depicted in Fig. 12(a) and Fig. 12(b), respectively. As pointed out before, the presence of metallic inclusions on top of the extremes of the stubs, at short distance, are revealed as dips in the measured envelope functions. In Fig. 12(a) the encoder is displaced with a nominal constant velocity of the 10 mm/s. As expected, the redundant clock signal ($Clock_2$) is advanced with regard to the clock signal ($Clock_1$). Therefore, the motion direction of the encoder can be inferred, and hence, the proper ID code can be extracted from the envelope function. Moreover, from adjacent pulses, the encoder velocity is found to be 10 mm/s, which is in excellent agreement with the considered nominal value. With regard to Fig. 12 (b), the encoder has been displaced over the sensitive part of the reader with a nominal constant acceleration of 3 mm/s^2. As can be seen, the encoder direction as well as the ID code (and hence the absolute position) can be inferred independently of the velocity of the encoder with regard to the sensitive part of the reader. Therefore, with the results obtained, it is clear that the functionality of the system is validated.

An important aspect in these encoders systems is the potential lack of alignment between the encoder and the reader. This aspect was studied in [16], where the effects of lateral misalignments between the encoder and the reader, as well as misalignments caused by rotation were considered. From that study, it was concluded that the system was tolerant to lateral shifts of the order of ±1 mm, and rotations of around ±3º. With these values, it seems feasible the use of the proposed systems in a real scenario.

III. Comparison with others synchronous approaches

A figure of merit in linear displacement/velocity sensors based on microwave encoders is the number of pulses per unit of length. Such figure of merit is directly related to the space resolution, and hence, directly related to the encoder period, i.e., 1.2 mm in our case. On the other hand, in chipless RFID systems, the density of information per surface (DPS) is one of the most important figures of merit. With such figure of merit, it is possible to compare different chipless RFID encoders as far as size is concerned. The higher the value of this parameter, the smaller the size of the encoder. Nevertheless, in the particular case of chipless-RFID systems based on near-field coupling and

TABLE I
Comparison of Different Synchronous Approaches

Ref.	Sync.	Direction detection	DPS (bits/cm^2)	DPL (bits/cm)
[53]	Yes	No	0.60	0.67
[54]	Yes	No	1.15	1.67
[55]	Yes	No	1.19	1.72
[56]	Yes	Yes	0.76	2.29
This work 1	**Yes**	**No**	**2.35**	**6.96**
This work 2	**Yes**	**Yes**	**1.63**	**6.96**

TABLE II
Comparative Analysis of Various Chipless-RFID Tags

Ref.	BW (GHz)	Bits	Area (cm^2)	DPF (bit/GHz)	DPS (bit/cm^2)	DPL (bits/cm)
Time-domain (Pulsed interrogation signal)						
[58]	---	4	59.4	---	0.07	0.02
[59]	0.05	2	---	40	---	0.10
[60]	---	4	---	---	---	0.06
[61]	---	8	---	---	---	0.20
[62]	0.8	5	26	6.25	0.19	0.19
[63]	---	2	70.0	---	0.03	---
[64]	---	2	8.75	---	0.23	---
Time-domain (Harmonic interrogation signal)						
[6]	*	40	5.40	*	7.40	3
[13]	*	80	9.44	*	8.47	3
[14]	*	100	20.4	*	4.90	16.7
[15]	*	100	13.4	*	7.46	16.7
[16]	*	100	3.84	*	26.0	16.7
[19]	*	15	9.04	*	1.66	2.99
This work 1	*	**16**	**6.81**	*	**2.35**	**6.96**
This work 2	*	**16**	**9.64**	*	**1.66**	**6.96**
Frequency-domain						
[22]	1	5	6.48	11.1	0.77	---
[24]	7.5	35	57.2	8.97	0.61	---
[26]	0.2	5	50.1	25.0	0.10	---
[29]	2	20	17.5	10.0	1.14	---
[30]	3.5	9	3.00	2.57	3.00	---
[31]	7.5	19	9.00	2.53	2.11	---
[33]	7	28.5	8.00	4.07	3.56	---
[34]	7.5	24	5.76	3.20	4.17	---
[39]	1.2	20	17.5	16.7	1.14	---
Hybrid						
[41]	5	22.9	8.00	4.58	2.86	---
[43]	6.4	64	10.9	10.0	5.88	---
[49]	1	16	6.75	16.0	2.37	---
[47]	3	9	7.20	3.00	1.25	---

* The spectral bandwidth of this approach is virtually null due to the fact that the interrogation signal is harmonic.

sequential bit reading, the most relevant parameter is the density of information per unit length (DPL), since, usually, the encoders are implemented as linear chains of inclusions (metallics in this case). Note that the DPL can be used to compare different approaches for the implementation of electromagnetic encoders, since the pulses, or dips, generated in the envelope function in linear displacement/velocity sensors can be interpreted as bits of information in chipless-RFID systems.

Table I compares the synchronous reader/encoder structures presented in this work with other approaches based on the same working principle, in terms of DPL and DPS. Another important aspect, also reflected in Table I, is the capability to detect the motion direction. As it can be seen, the prototype of Section II.B, able to discriminate the motion direction, exhibits a DPL which is more than 3 times the DPL of [56], and a DPS which is twice the DPS of [56]. It is important to mention that, to the best of our knowledge, [56] is the unique synchronous approach based on microwave encoders with direction detection capability in the literature. Regardless of this motion detection capability, the two prototypes presented in this paper, exhibit significantly higher DPL and DPS, in comparison to the other implementations indicated in Table I.

In the encoders of Table I, reading takes place synchronously, and such encoders can be useful as displacement/velocity sensors or as chipless-RFID tags based on near-field coupling and sequential bit reading. For this later functionality, it is also pertinent to extend the comparison of the system proposed in this paper with other chipless-RFID systems, including frequency-domain systems, hybrid systems and other time-domain based systems. Such comparison, indicated in Table II, is mainly based on the density of information per area unit, although other aspects are compared as well. As it can be seen, the proposed system is quite competitive for chipless-RFID applications, with a good combination of size, data capacity and performance. It should be taken into account that the introduction of motion direction detection capability and synchronous reading limits the information density. Nevertheless, good values have been obtained, and the system proposed in the paper is found to be competitive.

Concerning the advantages of motion direction detection capability of the proposed encoders in regard to application needs, let us mention that there are several applications that demand such capability. For instance, the determination of the position/velocity of conveyor belts or the cabin position/velocity in elevators systems can be done by properly encoding the belts (i.e., following a De Bruijn sequence). As mentioned, by reading a subsequence of the de Bruijn code, the absolute (or, more specifically, the quasi-absolute) position can be determined, but it is necessary to know the motion direction (since the sub-sequences of the ID code are not the same for both reading directions). Note also that the clock signal directly provides the velocity and the acceleration, if the velocity is not constant. In the application of the proposed approach as chipless-RFID system, the encoders (with a number of bits determined by the encoder length and period) equipped with synchronous reading capability and motion direction detection are more robust, since it is not necessary to know the displacement velocity of the tag over the reader (and indeed, it is not necessary that such velocity is constant). Moreover, knowing the motion direction of the tag avoids false readings, potentially caused by sequentially reading the ID code in the opposite direction to that which is intended.

CONCLUSIONS

In summary, high-resolution/high-density electromagnetic encoders based on linearly-shaped metallic inclusions with synchronous reading and motion direction detection capability have been reported. By synchronously reading the encoders, potential false readings of the ID code associated to eventual variations in the relative velocity between the encoder and the sensitive part of the reader, can be avoided. The system distinguishes the displacement direction of the encoder thanks to the presence of two clock chains in the encoder. This aspect is important to unambiguously identify the ID code of the encoder. Moreover, the absolute position of the encoder can be determined by using a Bruijn sequence in the encoder chain. The length and the period of the metallic inclusions, the key parameters in order to increase the density of information per unit length and surface of the encoders, have been significantly reduced, with regard to previous implementations based on a similar working principle. Specifically, the DPL and DPS has been found to be increased by a factor of three and two, respectively, as compared to other approaches with or without direction detection capability. It has been demonstrated that the proposed approach is useful for two applications: chipless-RFID systems based on near-field coupling with sequential bit reading, and linear displacement/velocity sensors. As a future work, the implementation of a switch at the input and output ports of the microstrip transmission line, controlled by a micro in order to sequentially fed the necessary interrogation signals (generated by a VCO) will be considered.

REFERENCES

[1] E. Eitel, “Basics of rotary encoders: overview and new technologies”, *Machine Design Magazine*, 7 May 2014.

[2] G. K. McMillan, D.M. Considine, Eds., *Process Instruments and Controls Handbook*, Fifth Edition, McGraw Hill 1999, ISBN 978-0-07-012582-7, page 5.26.

[3] X. Li, J. Qi, Q. Zhang, and Y. Zhang, “Bias-tunable dual-mode ultraviolet photodetectors for photoelectric tachometer,” *Appl. Phys. Lett*., vol. 104, no. 4, pp. 041108-1–041108-4, Jan. 2014.

[4] J. Naqui, F. Martín, “Application of broadside-coupled split ring resonator (BC-SRR) loaded transmission lines to the design of rotary encoders for space applications“, *IEEE MTT-S Int. Microw. Symp.* (IMS’16), San Francisco, May 2016.

[5] J. Mata-Contreras, C. Herrojo, and F. Martín, “Application of split ring resonator (SRR) loaded transmission lines to the design of angular displacement and velocity sensors for space applications”, *IEEE Trans. Microw. Theory Techn*., vol. 65, no. 11, pp. 4450-4460, Nov. 2017.

[6] C. Herrojo, J. Mata-Contreras, F. Paredes, F. Martín, “Microwave encoders for chipless RFID and angular velocity sensors based on S-shaped split ring resonators (S-SRRs)”, *IEEE Sensors J*., vol. 17, pp. 4805-4813, Aug. 2017.

[7] J. Mata-Contreras, C. Herrojo, and F. Martín, “Detecting the rotation direction in contactless angular velocity sensors implemented with rotors loaded with multiple chains of split ring resonators (SRRs)”, *IEEE Sensors J*., vol.18, no. 17, pp. 7055-7065, Sep. 2018.

[8] J. Mata-Contreras, C. Herrojo, F. Martín, “Electromagnetic rotary encoders based on split ring resonators (SRR) loaded microstrip lines”, *IEEE MTT-S Int. Microw. Symp.* (IMS’18), Philadelphia, Pennsylvania, Jun. 2018.

[9] F. Martín, C. Herrojo, J. Mata-Contreras, and F. Paredes, *Time-Domain Signature Barcodes for Chipless-RFID and Sensing Applications*, Springer, Cham, Switzerland, 2020.

[10] C. Herrojo, J. Mata-Contreras, F. Paredes, Ferran Martín, "Near-field chipless RFID system with high data capacity for security and authentication applications", *IEEE Trans. Microw. Theory Techn.*, vol. 65 (12), pp. 5298-5308, Dec. 2017.

[11] C. Herrojo, J. Mata-Contreras, F. Paredes, A. Núñez, E. Ramon, and F. Martín, "Near-field chipless-RFID system with erasable/programmable 40-bit tags inkjet printed on paper substrates", *IEEE Microw. Wireless Compon. Lett.*, vol. 28, pp. 272-274, March 2018.

[12] C. Herrojo, J. Mata-Contreras, F. Paredes, A. Núñez, E. Ramón, F. Martín, "Near-field chipless-RFID tags with sequential bit reading implemented in plastic substrates", *Int. J. Magnetism Magn. Mat.*, vol. 459 pp. 322–327, 2018.

[13] C. Herrojo, M. Moras, F. Paredes, A. Núñez, E. Ramón, J. Mata-Contreras, F. Martín, "Very low-cost 80-bit chipless-RFID tags inkjet printed on ordinary paper", *Technologies*, vol. 6, p. 52, 2018.

[14] J. Havlíček, C. Herrojo, F. Paredes, J. Mata-Contreras, F. Martín, "Enhancing the per-unit-length data density in near-field chipless-RFID systems with sequential bit reading", *IEEE Ant. Wireless Propag. Lett.*, vol. 18, pp. 89-92, Jan. 2019.

[15] C. Herrojo, F. Muela, J. Mata-Contreras, F. Paredes, F. Martín, "High-density microwave encoders for motion control and near-field chipless-RFID", *IEEE Sensors J.*, vol. 19, pp. 3673-3682, May 2019.

[16] C. Herrojo, F. Paredes, and F. Martín, "Double-stub loaded microstrip line reader for very high data density microwave encoders", *IEEE Trans. Microw. Theory Techn.*, vol. 67(9), pp. 3527-3536, Sep. 2019.

[17] C. Herrojo, F. Paredes, J. Mata-Contreras, F. Martín, "All-dielectric electromagnetic encoders based on permittivity contrast for displacement/velocity sensors and chipless-RFID tags*", IEEE-MTT-S Int. Microw. Symp.* (IMS'19), Boston (MA), USA, June 2019.

[18] C. Herrojo, F. Paredes, J. Mata-Contreras, E. Ramon, A. Núñez, F. Martín, "Time-domain signature barcodes: near-field chipless-RFID systems with high data capacity" *IEEE Microw. Mag.*, vol. 20, no. 12, pp. 87-101, Dec. 2019.

[19] C. Herrojo, F. Paredes, and F. Martín, "3D-printed high data-density electromagnetic encoders based on permittivity contrast for motion control and chipless-RFID", *IEEE Trans. Microw. Theory Techn*., published online, DOI: 10.1109/TMTT.2019.2963176.

[20] S. Preradovic and N. C. Karmakar, "Chipless RFID: bar code of the future," *IEEE Microw. Mag.*, vol. 11, pp. 87-97, 2010.

[21] S. Preradovic and N. C. Karmakar, *Multiresonator-Based Chipless RFID: Barcode of the Future*, Springer, 2011.

[22] I. Jalaly and I. D. Robertson, "RF barcodes using multiple frequency bands," *IEEE MTT-S Int. Microw. Symp.*, Long Beach, USA, Jun. 2005, pp. 139–142.

[23] S. Preradovic, I. Balbin, N. C. Karmakar, and G. Swiegers, "A novel chipless RFID system based on planar multiresonators for barcode replacement," 2008 *IEEE Int. Conf. RFID*, Apr. 2008, pp. 289–296.

[24] S. Preradovic, I. Balbin, N. C. Karmakar, and G. F. Swiegers, "Multiresonator-based chipless RFID system for low-cost item tracking," *IEEE Trans. Microw. Theory Techn.*, vol. 57, pp. 1411-1419, 2009.

[25] S. Preradovic and N. C. Karmakar, "Design of chipless RFID tag for operation on flexible laminates," *IEEE Anten. Wireless Propag. Lett.*, vol. 9, pp. 207-210, 2010.

[26] J. McVay, A. Hoorfar, and N. Engheta, "Space-filling curve RFID tags," *2006 IEEE Radio Wireless Symp.*, pp. 199–202.

[27] I. Jalaly and D. Robertson, "Capacitively-tuned split microstrip resonators for RFID barcodes," *2005 European Microwave Conference*, Oct. 2005, vol. 2, pp. 4–7.

[28] H.-S. Jang, W.-G. Lim, K.-S. Oh, S.-M. Moon, and J.-W. Yu, "Design of low-cost chipless system using printable chipless tag with electromagnetic code", *IEEE Microw. Wireless Compon. Lett.*, vol. 20, pp. 640-642, 2010.

[29] A. Vena, E. Perret, and S. Tedjini, "A fully printable chipless RFID tag with detuning correction technique", *IEEE Microw. Wireless Compon. Lett.*, vol. 22(4), pp. 209-211, 2012.

[30] A. Vena, E. Perret, and S. Tedjini, "Design of compact and auto-compensated single-layer chipless RFID tag", *IEEE Trans. Microw. Theory Techn*., vol. 60(9), pp. 2913-2924, Sep. 2012.

[31] A. Vena, E. Perret, and S. Tedjini, "High-capacity chipless RFID tag insensitive to the polarization", *IEEE Trans. Ant. Propag.*, vol. 60(10), pp. 4509-4515, Oct. 2012.

[32] D. Girbau, J. Lorenzo, A. Lazaro, C. Ferrater, and R. Villarino, "Frequency-coded chipless RFID tag based on dual-band resonators," *IEEE Ant. Wireless Propag. Lett*., vol. 11, pp. 126–128, 2012.

[33] M. M. Khan, F. A. Tahir, M. F. Farooqui, A. Shamim, H. M. Cheema, "3.56-bits/cm^2 compact inkjet printed and application specific chipless RFID tag," *IEEE Ant. Wireless Propag. Lett*., vol. 15, pp. 1109-1112, 2016.

[34] R. Rezaiesarlak and M. Manteghi, "Complex-natural-resonance-based design of chipless RFID tag for high-density data," *IEEE Trans. Ant. Propag*., vol. 62, pp. 898-904, Feb. 2014.

[35] M. S. Bhuiyan and N. Karmakar, "A spectrally efficient chipless RFID tag based on split-wheel resonator," in *Int. Antenna Technol. Workshop on Small Antennas, Novel EM Struct., Mater., Appl*., 2014, pp. 1–4.

[36] C. M. Nijas *et al*., "Low-cost multiple-bit encoded chipless RFID tag using stepped impedance resonator," *IEEE Trans. Ant. Propag*., vol. 62, no. 9, pp. 4762–4770, Sep. 2014.

[37] J. Machac and M. Polivka, "Influence of mutual coupling on performance of small scatterers for chipless RFID tags," *24th Int. Radioelektron. Conf*., 2014, pp. 1–4.

[38] M. Khaliel, A. El-Awamry, A. Fawky, M. El-Hadidy, and T. Kaiser, "A novel co/cross-polarizing chipless RFID tags for high coding capacity and robust detection," *2015 IEEE Int. Symp. Ant. Propag. & USNC/URSI National Radio Sci. Meeting*, Jul. 2015, pp. 159–160.

[39] M. Svanda, J. Machac, M. Polivka, J. Havlicek., "A comparison of two ways to reducing the mutual coupling of chipless RFID tag scatterers," in Proc. of *21st International Conference on Microwave, Radar and Wireless Communications (MIKON)*, May 2016, pp. 1-4.

[40] C. Herrojo, J. Naqui, F. Paredes and F. Martín, "Spectral signature barcodes based on S-shaped Split ring resonators (S-SRR)", *EPJ Applied Metamaterials*, vol. 3, pp. 1-6, Jun. 2016.

[41] A. Vena, E. Perret, S. Tedjini, "Chipless RFID tag using hybrid coding technique," *IEEE Trans. Microw. Theory Techn.*, vol. 59, pp. 3356-3364, Dec. 2011.

[42] A. Vena, E. Perret, S. Tedjini, "A compact chipless RFID tag using polarization diversity for encoding and sensing", *2012 IEEE Int. Conf. RFID*, pp. 191-197, 2012.

[43] M. A. Islam and N. C. Karmakar, "A novel compact printable dual-polarized chipless RFID system," *IEEE Trans. Microw. Theory Techn.*, vol. 60, pp. 2142-2151, Jul. 2012.

[44] I. Balbin, N.C. Karmakar, "Phase-encoded chipless RFID transponder for large scale low cost applications", *IEEE Microw. Wireless. Compon. Lett.*, vol. 19, pp. 509-511, 2009.

[45] S. Genovesi, F. Costa, A. Monorchio, G. Manara, "Chipless RFID tag exploiting multifrequency delta-phase quantization encoding", *IEEE Ant. Wireless Propag. Lett.*, vol. 15, pp. 738-741, 2015.

[46] O. Rance, R. Siragusa, P. Lemaitre-Auger, and E. Perret, "RCS magnitude coding for chipless RFID based on depolarizing tag," in *IEEE MTT-S Int. Microw. Symp. Dig*., 2015, pp. 1–4.

[47] C. Herrojo, F. Paredes, J. Mata-Contreras, S. Zuffanelli and F. Martín, "Multi-state multi-resonator spectral signature barcodes implemented by means of S-shaped split ring resonators (S-SRR)", *IEEE Trans. Microw. Theory Techn.*, vol. 65, no. 7, pp. 2341-2352, Jul. 2017.

[48] C. Herrojo, J. Naqui, F. Paredes, F. Martín, "Spectral signature barcodes implemented by multi-state multi-resonator circuits for chipless RFID tags", *IEEE MTT-S Int. Microw. Symp.* (IMS'16), San Francisco, May 2016.

[49] O. Rance, R. Siragusa, P. Lemaître-Auger, E. Perret, "Toward RCS magnitude level coding for chipless RFID," *IEEE Trans. Microw. Theory Techn.*, vol. 64, pp. 2315-2325, Jul. 2016.

[50] C. Feng, W. Zhang, L. Li, L. Han, X. Chen, and R. Ma, "Angle-based chipless RFID tag with high capacity and insensitivity to polarization," *IEEE Trans. Ant. Propag*., vol. 63, no. 4, pp. 1789–1797, Apr. 2015.

[51] A. El-Awamry, M. Khaliel, A. Fawky, M. El-Hadidy, and T. Kaiser, "Novel notch modulation algorithm for enhancing the chipless RFID tags coding capacity," in *IEEE Int. RFID Conf*., 2015, pp. 25–31.

[52] A. Vena, A. A. Babar, L. Sydanheimo, M. M. Tentzeris, and L. Ukkonen, "A novel near-transparent ASK-reconfigurable inkjet-printed chipless RFID tag," *IEEE Ant. Wireless Propag. Lett*., vol. 12, pp. 753–756, 2013.

[53] F. Paredes, C. Herrojo, and F. Martin, "An approach for Synchronous Reading of Near-Field Chipless-RFID Tags", *10th IEEE International Conference on RFID Technology and Applications* (IEEE RFID-TA 2019), Pisa, Italy, 25-27 Sep. 2019.

[54] F. Paredes, C. Herrojo, and F. Martín, "High Data Density Near-Field Chipless-RFID Tags with Synchronous Reading", *IEEE Journal of RFID*, published as early access.

[55] F. Paredes, C. Herrojo, and F. Martín, "Microwave Encoders with Synchronous Reading and Direction Detection for Motion Control Applications", *URSI GASS 2020*, Rome, Italy, 29-5 Aug., 2020.

[56] F. Paredes, C. Herrojo, and F. Martín, "Chipless-RFID Sensors for Motion Control Applications", *2020 IEEE-MTT-S Int. Microw. Symp.* (IMS'20), Los Angeles, CA, USA, 21-26 Jun., 2020.
[57] N.C. de Bruijn, ""Acknowledgement of Priority to C. Flye Sainte- Marie on the counting of circular arrangements of 2n zeros and ones that show each n-letter word exactly once", *T.H.-Report 75-WSK-06*, Technological University Eindhoven, 1975.
[58] A. Chamarti and K. Varahramyan, "Transmission delay line based ID generation circuit for RFID applications," *IEEE Microw. Wireless Compon. Lett.*, vol. 16, pp. 588-590, 2006.
[59] F.J. Herraiz-Martínez, F. Paredes, G. Zamora, F. Martín, and J. Bonache, "Printed magnetoinductive-wave (MIW) delay lines for chipless RFID applications", *IEEE Trans. Ant. Propag.*, vol. 60, pp. 5075-5082, Nov. 2012.
[60] L. Zhang, S. Rodriguez, H. Tenhunen, and L.-R. Zheng, "An innovative fully printable RFID technology based on high speed time-domain reflections," in *Conference on High Density Microsystem Design and Packaging and Component Failure Analysis, 2006. HDP'06*., Shanghai, China, Jun. 2006, pp. 166–170.
[61] L. Zheng, S. Rodriguez, L. Zhang, B. Shao, and L.-R. Zheng, "Design and implementation of a fully reconfigurable chipless RFID tag using Inkjet printing technology," in *2008 IEEE International Symposium on Circuits and Systems*, Seattle, USA, May 2008, pp. 1524–1527.
[62] C. Mandel, M. Schussler, M. Maasch, and R. Jakoby, "A novel passive phase modulator based on LH delay lines for chipless microwave RFID applications," in *2009 IEEE MTT-S International Microwave Workshop on Wireless Sensing, Local Positioning, and RFID*, Cavtat, Croatia, Sep. 2009, pp. 1–4.
[63] R. Nair, E. Perret, and S. Tedjini, "Temporal multi-frequency encoding technique for chipless RFID applications," in *IEEE MTT-S International Microwave Symposium Digest*, Montreal, Canada, Jun. 2012, pp. 1–3.
[64] R. Nair, E. Perret, and S. Tedjini, "Chipless RFID based on group delay encoding," in *IEEE Int. RFID-Technol. Appl. Conf.*, 2011, pp. 214–218.

C. Herrojo was born in Barcelona, Spain, in 1983. He received the Telecommunications Technical Engineering degree in electronic systems and Telecommunications Engineering degree from the Universitat Autònoma de Barcelona in 2010 and 2012, respectively and the PhD degree in Electronics Engineering from the same university in 2018. His research interests include RF/microwave devices, Chipless-RFID and RFID technology, and Metamaterials.

F. Paredes was born in Badalona (Barcelona), Spain in 1983. He received the Telecommunications Engineering Diploma (specializing in Electronics) and the Telecommunications Engineering degree from the Universitat Autònoma de Barcelona in 2004 and 2006, respectively and the PhD degree in Electronics Engineering from the same university in 2012. He was Assistant Professor from 2006 to 2008 at the Universitat Autònoma de Barcelona, where he is currently working as a Research Assistant. His research interests include metamaterial concepts, passive microwaves devices, antennas and RFID.

F. Martín (M'04-SM'08-F'12) was born in Barakaldo (Vizcaya), Spain in 1965. He received the B.S. Degree in Physics from the Universitat Autònoma de Barcelona (UAB) in 1988 and the PhD degree in 1992. From 1994 up to 2006 he was Associate Professor in Electronics at the Departament d'Enginyeria Electrònica (Universitat Autònoma de Barcelona), and since 2007 he is Full Professor of Electronics. In recent years, he has been involved in different research activities including modelling and simulation of electron devices for high frequency applications, millimeter wave and THz generation systems, and the application of electromagnetic bandgaps to microwave and millimeter wave circuits. He is now very active in the field of metamaterials and their application to the miniaturization and optimization of microwave circuits and antennas. Other topics of interest include microwave sensors and RFID systems, with special emphasis on the development of high data capacity chipless-RFID tags. He is the head of the Microwave Engineering, Metamaterials and Antennas Group (GEMMA Group) at UAB, and director of CIMITEC, a research Center on Metamaterials supported by TECNIO (Generalitat de Catalunya). He has organized several international events related to metamaterials and related topics, including Workshops at the IEEE International Microwave Symposium (years 2005 and 2007) and European Microwave Conference (2009, 2015 and 2017), and the Fifth International Congress on Advanced Electromagnetic Materials in Microwaves and Optics (Metamaterials 2011), where he acted as Chair of the Local Organizing Committee. He has acted as Guest Editor for six Special Issues on metamaterials and sensors in five International Journals. He has authored and co-authored over 600 technical conference, letter, journal papers and book chapters, he is co-author of the book on Metamaterials entitled *Metamaterials with Negative Parameters: Theory, Design and Microwave Applications* (John Wiley & Sons Inc.), author of the book *Artificial Transmission Lines for RF and Microwave Applications* (John Wiley & Sons Inc.), co-editor of the book *Balanced Microwave Filters* (Wiley/IEEE Press) and co-author of the book *Time-Domain Signature Barcodes for Chipless-RFID and Sensing Applications* (Springer). Ferran Martín has generated 21 PhDs, has filed several patents on metamaterials and has headed several Development Contracts.

Prof. Martín is a member of the IEEE Microwave Theory and Techniques Society (IEEE MTT-S). He is reviewer of the IEEE Transactions on Microwave Theory and Techniques and IEEE Microwave and Wireless Components Letters, among many other journals, and he serves as member of the Editorial Board of IET Microwaves, Antennas and Propagation, International Journal of RF and Microwave Computer-Aided Engineering, and Sensors. He is also a member of the Technical Committees of the European Microwave Conference (EuMC) and International Congress on Advanced Electromagnetic Materials in Microwaves and Optics (Metamaterials). Among his distinctions, Ferran Martín has received the 2006 Duran Farell Prize for Technological Research, he holds the *Parc de Recerca UAB – Santander* Technology Transfer Chair, and he has been the recipient of three ICREA ACADEMIA Awards (calls 2008, 2013 and 2018). He is Fellow of the IEEE and Fellow of the IET.